

The Specific of the Creep Process in Hydrogen of the Degraded in Service 2.25Cr-Mo Steel

Andrzej Zagórski^{1,a}, Oleksandra Student^{2,b}, Leontiy Babiy^{3,c},
Hryhoriy Nykyforchyn^{4,d} and Krzysztof Kurzydłowski^{5,e}

^{1,5}Warsaw University of Technology, Faculty of Materials Science & Engineering,
Wolowska 141, 02-507 Warsaw, Poland

^{2,3,4}Karpenko Physico-Mechanical Institute of the National Academy of Sciences of Ukraine,
Departure of Corrosion-Hydrogen Degradation and Material Protection,
5 Naukova, 79601 Lviv, Ukraine

^aandrzej.zagorski@inmat.pw.edu.pl, ^aa.zagorski@metroup.pl, ^bstudent@ipm.lviv.ua,
^cleontiy@ipm.lviv.ua, ^dnykyfor@ipm.lviv.ua, ^ekjk@inmat.pw.edu.pl

Keywords: 2.25Cr-Mo steel, oil hydrocracking process, virgin state metal, degraded metal, secondary creep rate, hydrogen.

Abstract. Stability of the mechanical properties of the steel of the oil hydrocracking reactor body during long-term exploitation is very important to guarantee its safe service. That's why it is very significant to know metal properties after different service life for prediction of the material workability.

The effect of hydrogenation on steady state creep of the 2.25Cr-Mo steel in virgin state and after service in oil hydrocracking reactor was shown. It was revealed that a secondary creep rate in hydrogen is higher than in air for the steel in virgin state and after service. Firstly it means that initial steel properties during service are exhausted. Secondly it means that hydrogen simultaneously effects at the degradation and creep processes. The hydrogen intensifies the diffusion process and consequently accelerates the steel degradation and makes easy the creep process.

The mechanism of hydrogen effect is revealed. It is shown that tests in hydrogen do the systems of sliding more active and thus provides localization of the creep process. Fractography features of fracture during testing in hydrogen and in air of the 2.25Cr-Mo steel in virgin state are presented.

Introduction

Hydrocracking is an exothermal process. Heat from the reaction zone is taken off due to hydrogen with the partial pressure ~3...3.5 MPa. The vessels of oil hydrocracking reactors are usually manufactured from heat-resistant 2.25Cr-Mo steel and their internal surface is protected against corrosion by austenitic stainless steel cladding. The final thermal treatment of these structural elements with corrosion-resistant cladding occurs at a temperature of 690°C [1, 2]. Stability of the mechanical properties of this steel during long-term exploitation is very important to guarantee serviceability of oil hydrocracking reactor. First of all the damage of such reactors is very dangerous for service staff and environment. Due to high parameters of processing environment (temperature ~450 °C and pressure ~ 15 MPa) and large external dimensions of the reactor (diameter up to 4 m, wall thickness up to 0.25 m and height ~20 m) the damage of the reactor causes large scale destructions [3]. And, secondly, the reactor damage is very expensive because of appreciably increasing maintenance costs and especially through very high costs for clearing consequence of accidents.

It is well known that vessel steels are intensively hydrogenated in such service regimes. Additionally, a sharp temperature decrease certainly retards hydrogen diffusion. Diffusivity of

hydrogen in α -iron decreases from 10^{-4} to $4.4 \cdot 10^{-5} \text{ cm}^2/\text{s}$ with a temperature change from 450°C to 100°C [4-6]. At the same time the nonequilibrium concentration of absorbed hydrogen is fixed by metal and reaches 0.9 g/cm^3 , contrary to 0.1 g/cm^3 for α -iron at ambient temperature [7]. The redundant hydrogen deforms of α -iron crystal lattice, creates internal stresses, aims for structural damages at the grain and phase boundaries, dislocations and so on [8]. All of these factors promote the damages origin and degradation of mechanical properties of the vessel metal [9] which are not always take into account due to estimation of the design lifetime of oil hydrocracking reactors.

In addition, the high temperature and pressure in reactor create the favorable conditions for a vessel steel creep. Operating experience shows that creep resistance of material is changed due to, firstly, degradation of metal during long-term service and, secondly, due to the influence of technological environment ($\sim 20\%$ of hydrogen) on both process (degradation and creep as well). It is possible to reveal the simultaneous effect of high temperature and hydrogen on the intensity of metal degradation. Besides, by comparing creep strain rate in air and hydrogen, it is possible to show the effect of hydrogenation environment on metal creep in virgin state and after service.

The aim of the paper is to reveal the peculiarities of creep mechanism in hydrogen and regularity of hydrogen effect on the creep strain rate in dependence of the load level for the vessel 2.25Cr-Mo steel in virgin state and after $\sim 6 \cdot 10^4 \text{ h}$ of service in oil hydrocracking reactor as the “witness-specimens” and compare them with creep strain rate for the vessel 15KH2MFA steel in virgin state.

Methodical Aspects

Two vessel steels (15KH2MFA and 2.25Cr-Mo) in virgin state were tested. In addition the 2.25Cr-Mo steel was tested after $\sim 6 \cdot 10^4 \text{ h}$ of holding inside the oil hydrocracking reactor as the “witness-specimen”. The chemical composition of the tested steels are presented in Table 1.

Table 1. The chemical composition tested steels

Steel	C	Mn	Si	P	S	Cr	Ni	Cu	Mo	Al	V	Ca	Sn
2.25Cr-Mo	0.14	0.58	0.19	0.006	0.003	2.16	0.10	0.040	1.00	0.02	0.010	-	0.014
15KH2MFA	0.15	0.5	0.3	0.012	0.015	2.8	0.4	0.1	0.7	-	0.27	0.025	-

The creep tests were carried out in accordance with the method developed for the accelerated degradation of steels in laboratory conditions [10-13] and allow us to test the material at service temperature in gaseous environments. The specimens were loaded using the two-position device AIMA-5-1 with a strain rate of the specimen of about $2 \cdot 10^{-6} \text{ s}^{-1}$ up to selected initial stress level σ_0 . The specimens load levels during creep testing were kept constant. The specimens were tested in vacuum chambers filled with hydrogen under the pressure up to 0.5 MPa. The cross-section and effective length of used specimens were 20x3 mm and 25 mm correspondingly. The specimens disposed inside of chamber were heated by electric furnace disposed around of the chamber. The load values F versus elongation of the specimen values δ were measured by gauges located from outside of the chamber. The diagrams $F - \delta$ were registered during active loading of specimens. The thermocouples were disposed outside of the chambers. They were preliminarily calibrated with respect to the thermocouples disposed on the mean level of the effective length of specimens inside the chambers. The time variation of values δ , F and test temperature T was controlled during test and accumulated as the data base for farther analysis.

Fractography investigations of the fracture surfaces and slip bands on side surfaces of specimens subjected to creep testing were carried out on the scanning electron microscope HITACHI S-2600N.

Experimental Results and Analysis

The creep tests at sustained loading at a temperature of 450 °C revealed an ambiguous character of the creep curve position after tests in air (curve 1) and in hydrogen (curve 2, Fig. 1a). In spite of the same load level during the creep test in both environments, curve 2 is placed below curve 1. It is the consequence of the different creep intensity in air and in hydrogen. At the tertiary creep curve 2 obtained in hydrogen crosses curve 1 for air because of the additional intensification of creep in hydrogen. Finally, elongation of the specimen the moment of fracture is lower for test in hydrogen. Such a tendency of hydrogen effect was also confirmed at other stress levels σ_0 . The revealed effect is caused by the different secondary creep rate v_{II} of the metal in air and in hydrogen (Fig. 1b). So, the steady-state creep rate is higher for the test in hydrogen independently of the σ_0 level but this effect is more visible if the σ_0 level is lower. In particular the values v_{II} in the hydrogen were by a factor of 2.5 and 5.4 higher then in air at $\sigma_0 = 520$ MPa and 500 MPa correspondingly. Therefore environment effect may be some more higher at the considerably lower operation stress arising in the reactor vessel during hydrocracking process. It's important to take into account the hydrogen effect in the reactor lifetime estimation.

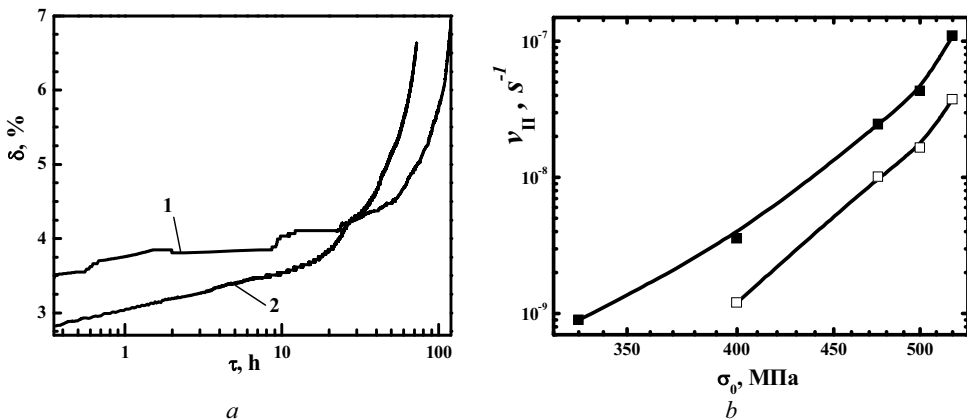


Fig. 1. Creep curves in air (1) and in hydrogen (2) at the initial stress level $\sigma_0 = 520$ MPa (a) and secondary creep rate v_{II} versus σ_0 level curves in air (light) and in hydrogen (dark symbols) (b) for 2.25Cr-Mo steel in virgin state at 450 °C.

The thick oxide film is formed at the surface of specimens tested in air but practically did not formed in hydrogen. This film prevents dislocations getting out of on the specimen surface and, thus, retards the deformation process in air. This feature explains the smaller secondary creep rate v_{II} for metal tested in air than in hydrogen.

The analysis of density and morphology of the slip bands on the wider specimen side allow us to observe all stages of deformation up to fracture. Thus, sliding traces are practically absent on the part close to the specimen fillets but farther from them they appears one by one only. They do not cross the boundaries of the separate grains. It is the main feature of the uniform creep. Sliding traces were observed only in the most favorable oriented grains relative to the external stresses. These traces are not homogeneous. It is clear that density and relief of sliding traces increase when approaching the fracture surface both of specimens tested in air and in hydrogen.

Generally macroshear character of fracture of the specimens tested in air and in hydrogen were observed. Thus fracture surfaces of all tested specimens were oriented along the tangential stress (Fig. 2 a, Fig. 2 b). At the same time the profiles of the fracture surfaces were also oriented along tangential stress but only at high σ_0 . At low σ_0 they are oriented practically transversely to the external stresses. In hydrogen this process takes place at higher stress level in comparison with air.

Discontinuities of oxide film on the surfaces of specimens tested in air was mainly oriented transversely to the external loading. The dense netting of the slip band traces oriented along and across the direction of tensile stress were observed in the field of oxide film breaking near the fracture surface (Fig. 2 *c*).

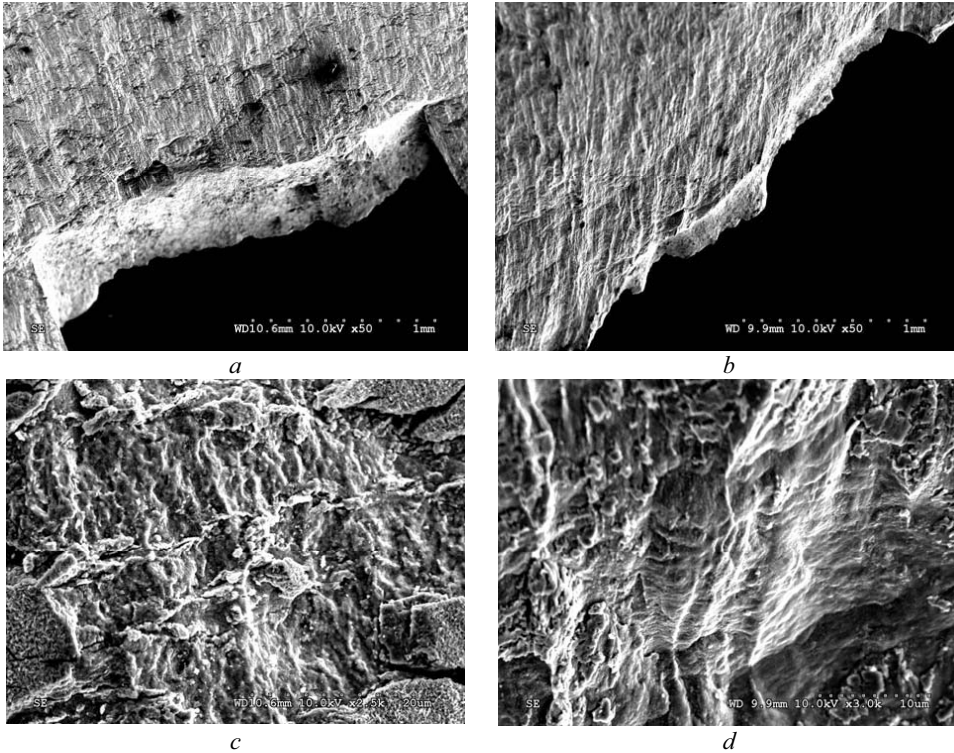


Fig. 2. SEM of the sliding traces on the wide side of 2.25Cr-Mo steel specimens in virgin state after creep test at 450 °C and $\sigma_0 = 520$ MPa in air (*a, c*) and in hydrogen (*b, d*). The axes of specimens are clock-oriented from 17 h to 11 h and from 18 h to 12 h on the left and right pictures, correspondingly.

The macrofeatures of fracture during creep testing in hydrogen changed. Firstly, in spite of practically shear character of fracture near the side surfaces of specimens the narrow strip in the midpoint of surfaces fracture with another orientation was noticed. Secondly, another orientation and density of slip bands was observed on the specimen side surfaces (Fig. 2 *d*). The absence of oxidation increases the information ability of slip bands. First of all, essentially more of its density and relief were noticed nearby the fracture surface. The additional sliding systems were revealed oriented in the direction of the tangent stresses action. At high levels of loading one of the sliding systems is dominating nearby the specimen neck. It defines the orientation of fracture profiles along the direction of effective circumferential stress (Fig. 2 *b*). At lower values of σ_0 all sliding systems became more active and equivalent. This causes a more frequent crossing of the slip bands and make difficulties for dislocations motion. It is typical for tests in air. Due to high hydrogen mobility it is possible the unlocking of dislocations motion. As a result a more intensive relief on the side surfaces of specimens tested in hydrogen is seen (Fig. 2 *d*). Localization of deformation in hydrogen occurs faster than in air too and this explains higher rate of steady-state creep in hydrogen.

The comparison of the investigation results for 2.25 Cr-1Mo steel in virgin state and after holding in service conditions shows that independently of material state and σ_0 levels, a steady-state creep

rate v_{II} is essentially higher in hydrogen than in air (Fig. 3). This result is extremely important when calculating workability and life time of such structures as oil hydrocracking reactors. Whereas, to this time creep test data obtained in air were usually taken into account for such calculation.

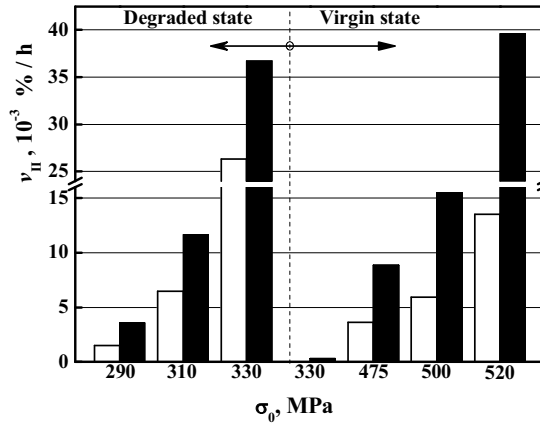


Fig. 3. The bar graphs of steady-state creep rate v_{II} at different initial levels of stresses σ_0 obtained at a temperature of 450 °C in air (white) and in hydrogen (black bars) for the 2.25Cr-Mo steel in virgin state and after $\sim 6 \cdot 10^4$ h holding inside the oil hydrocracking reactor as “specimen-witness”.

The next important conclusion obtained from Fig. 3 is that the same levels of steady-state creep rates in hydrogen for the steel in virgin state and after service are reached at different stress levels. These levels are essentially lower for the degraded metal in comparison with metal in virgin state. This effect is particularly evident at high stress levels. As a result the v_{II} rate in hydrogen at the same level of σ_0 (in particular at 330 MPa) for the steel after service is essentially higher (more than in 35 times) in comparison with the steel in virgin state. The creep process is not observed in the air at the same stress level during the six month creep test. In this respect it is very important to take into account the hydrogen effect, especially for steel degraded during long-term service.

The essential hydrogen effect on the specimens durability τ at different stress levels σ_0 is revealed at different creep strain levels (Fig. 4 a). It means that hydrogen effect appears independently of the stress levels. The last result is very significant to be taken into account during estimation of reactor lifetime. The real stresses in the wall body of the oil hydrocracking reactor are usually less than σ_0 used in the laboratory creep test. Therefore obtained data may be extrapolate for the real running hours of reactor and allows us to estimate the dangerous stress level taking into account the hydrogen effect.

The effect of steel degradation during its long-time holding in the reactor is appreciable greater than hydrogen effect (Fig. 4 b). It means that it is very important to take into account the degradation effect during calculation of the residual life-time of such significant structures as oil hydrocracking reactors. It is necessary to consider that the body of the oil hydrocracking reactor is subjected to stress. Therefore a more strong degradation effect will be expected for the steel exploited under real stress conditions in comparison with ones operate as the “specimen-witness”.

Comparison of the stable creep rate v_{II} values obtained in hydrogen at temperature 450 °C at different stress levels σ_0 for the 15Kh2MFA and 2.25Cr-1Mo steels testify to appreciably worse creep properties of the 15Kh2MFA steel in comparison to the 2.25Cr-1Mo steel in virgin state (Fig. 5). Perhaps it is a result of a very high content of sulfur and phosphorus in the first steel. It is well known that the higher content of these elements decrease essentially the serviceability of steels during long time exploitation at high temperatures. Moreover the stable creep rate values of the

2.25Cr-1Mo steel after $\sim 6 \cdot 10^4$ h holding inside the oil hydrocracking reactor as “specimen-witness” would be a little bit worse than of the 15Kh2MFA steel in virgin state at the suitable stress levels.

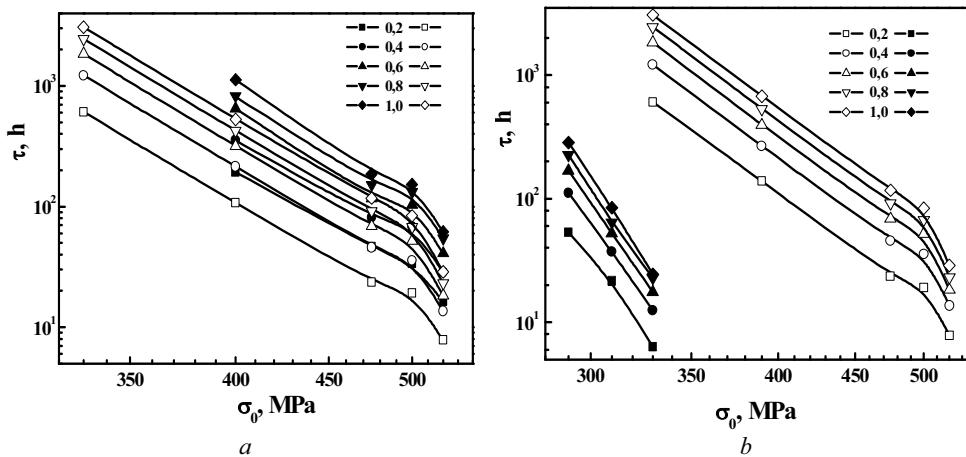


Fig. 4. The creep rupture strength curves $\tau - \sigma_0$ at different strain levels (numerals besides symbols correspond to strain levels in percentage terms) at a temperature of 450 °C in hydrogen (white) and in air (black symbols) of the 2.25Cr-Mo steel in virgin state (a and b, white symbols) and after $\sim 6 \cdot 10^4$ h of its holding inside the oil hydrocracking reactor as witness specimen (b, black symbols).

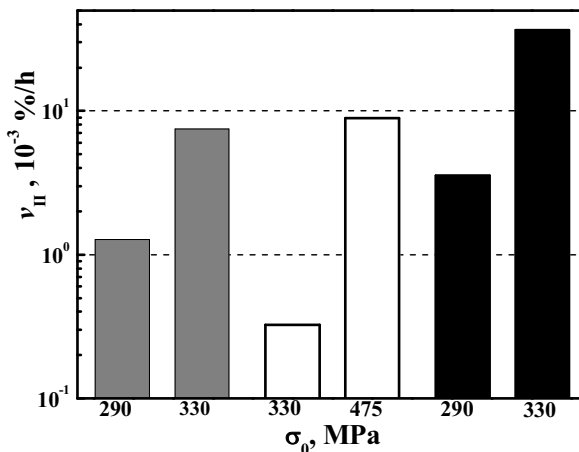


Fig. 5. The stable creep rate ν_{II} at different stress levels σ_0 for the 15Kh2MFA (grey) and 2.25Cr-1Mo (white, black) steels before (grey, white) and after $\sim 6 \cdot 10^4$ h holding inside the oil hydrocracking reactor as the “specimen-witness” [14, 15] (black bars) obtained in hydrogen at a temperature of 450 °C.

Fractography investigations of the fracture surface of the specimens after creep in air and in hydrogen testify to the fact that the general mechanism of fracture is classical ductile. It is realized by the initiation, growth and coalescence of microvoids with formation of the dimple structure (Fig. 5). The fracture by shear prevails independently of the environment type (Fig. 5 a, b). Here the dimples are not deep but strongly elongated and their contours are not clear (Fig. 5 c). However dimples become well-defined, different by size and practically equiaxial on the central parts of the fracture surfaces (Fig. 5 e, d). It testifies that normal stresses are substantially responsible for their origin.

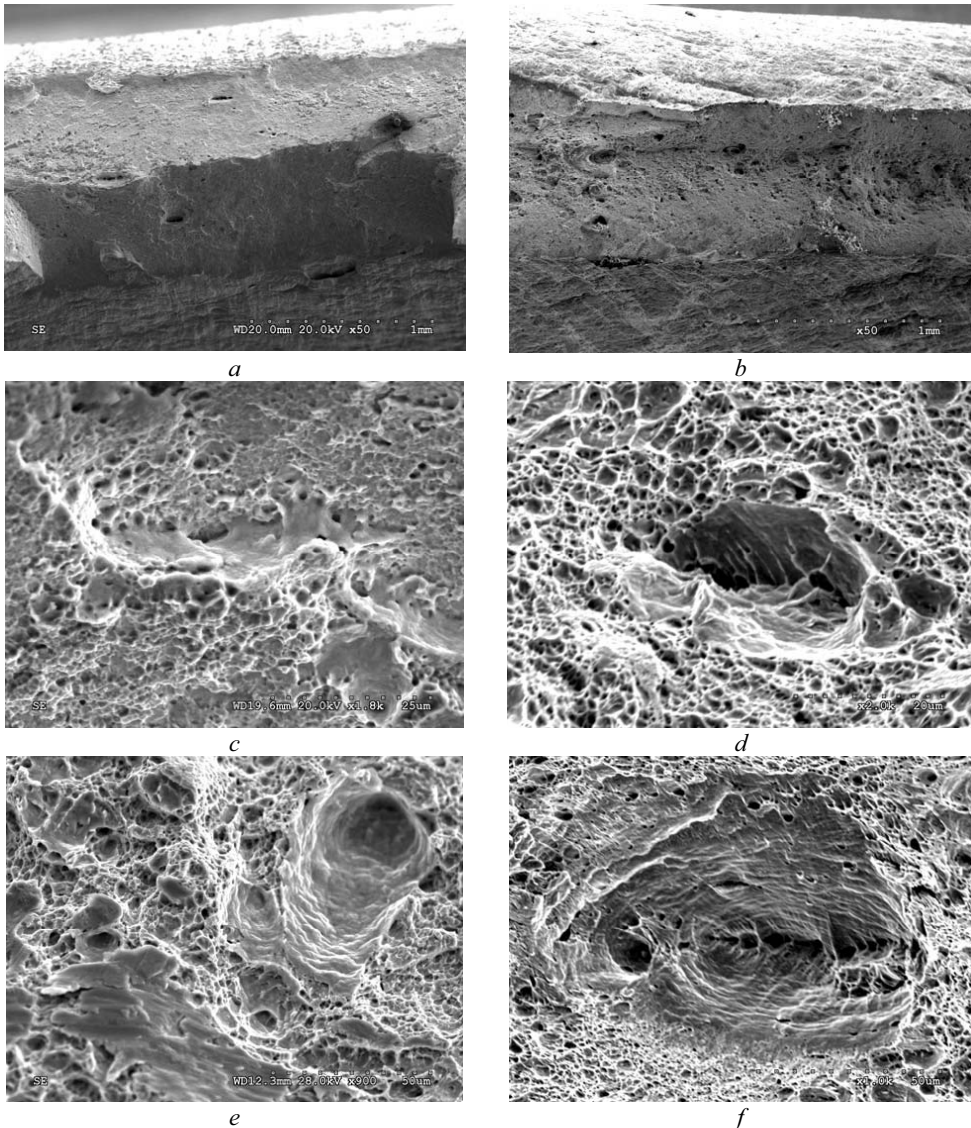


Fig. 5. SEM of the fracture surfaces of the 2.25Cr-Mo steel in the virgin state tested in air (*a, c, e*) or in hydrogen (*b, d, f*) at a temperature of 450 °C and 520 (*a, c, e*) or 475 MPa (*b, d, f*) stress levels.

Especially fractography peculiarities were revealed after tests in hydrogen (Fig. 5 *d, f*). In spite of the shear character of fracture surface at macro level, the narrow strips in the central part of its with high density of the big dimples are shown. Their sizes change within the range from 20 μm to 200 μm (Fig. 5 *b*). Fracture surface in hydrogen seems more brittle at macro level in comparison with tests in air due to central part of the fracture surface which is practically normal oriented. At higher magnification the line-up from the smaller dimples is recognized on the bottom of big voids (Fig. 5 *d, f*). It is shown that bridges between neighbouring small dimples are broken forming specific “moustache” like traces due to symmetric divergent edges. Furthermore the generative surfaces of big voids are covered with the sliding

traces. They do not differ from the ones observed on the wide side of the specimen surface (Fig. 5.f). All these features could testify that big voids grow by a coalescence of hydrogen-filled small voids. The last ones can promote big void growth because of the internal pressure increase. So, not only voids located directly in fracture are going to take part in fracture process, which is typical for tests in air, but also the voids located in the subsurface layers, and it makes fracture in hydrogen easier. Summing up the fractography features, one can state that, in spite of the common ductile character of fracture in air and in hydrogen, density of voids and dimples in the last case is essentially higher. Furthermore, small voids are more flat after tests in hydrogen and unusual voids growth is observed. The mentioned peculiarities show that lower power-consuming of fracture in hydrogen, and this agree well with the results of creep tests.

Conclusions

1. Steady-state creep rate of the 2.25Cr-Mo steel in virgin state and after degradation in-service conditions is higher in hydrogen than in air.
2. The degradation of the 2.25Cr-Mo steel after $\sim 6 \cdot 10^4$ h holding inside the oil hydrocracking reactor as the “specimen-witness” essentially decrease its serviceability in both environments and at all initial stress levels.
3. The high density of the big dimples are revealed at the specimens tested in hydrogen. At higher magnification the line-up from the smaller dimples is shown on the bottom of big voids. It is assumed that big voids grow by a coalescence of hydrogen-filled small voids.

References

- [1] Ohniski K., Chiba R., Watanabe Y. et. al. in: Hydrogen induced disbonding of stainless steel overlay weld. – N.Y.: Pressure Vessels Research Committee Meeting (1980).
- [2] Imanaka T., Shimomura J., Nakano S. and Yasuda K.: Kawasaki Steel Techn. Rep. 13 (1985), p. 109-119.
- [3] Panasyuk V.V., Andreykiv O.Y. and Gembara O.V.: Int. J. Hydrogen Energy. 25/1 (2000), p. 67-74.
- [4] Geller W. and Sun T.: Arch. Eisenhüttenw. 21 (1950), p. 423-430.
- [5] Johnson E.W. and Hill M.L.: Trans. AIME. 218 (1960), p. 1104-1112.
- [6] Hobson J.D.: JISI 189 (1958), p. 315-321.
- [7] Metal Handbook, ASM International. Metal Park, OH, (1948).
- [8] Student O.Z. and Loniuk B.P.: Materials Science. 33, N6 (1997), p. 865-866.
- [9] Student O.Z. and Loniuk B.P.: Materials Science. 33, N4 (1997), p. 532-538.
- [10] Nykyforchyn G.M. and Student O.Z. in: Proc. 12th Biennial Conf. Fract. - ECF12 “Fracture from defects” / Eds. M.W. Brown, E.R. de los Rios and K.J. Miller, London: EMAS V.III. (1998), p.1139-1144.
- [11] Student O.Z. : Material Science. 34, N4 (1998), p. 497-507.
- [12] Nykyforchyn H., Loniuk B., Student O. and Zuidema J. in: Proc. European Symp. on Pressure Equipment – ESOPÉ 2001, Paris, Assoc. Francaise Ing. Appareils a Pression, (2001), p. 697-708.
- [13] Kurzydłowski K.J. and Nykyforchyn H.: Problemy Eksploatacji 51/4 (2003). p. 7- 18.
- [14] Babij L., Zagórski A. and Student O.: Phys.-Chem. Mech. Mater. V.1., Spec. Issue 5 (2006). p. 227-232.
- [15] Babij L., Student O. and Zagórski A.: Phys.-Chem. Mech. Mater. V.1., Spec. Issue 6 (2008). p. 100-105. (in Ukrainian).